ADVANCED MATERIALS

of the PSS concentration, amount of loading, and number of loading cycles. This method of nanocrystal preparation and stabilization might be applicable to other materials, which form complexes by electrostatic interactions with polyelectrolytes, as well as insoluble crystals having a larger stability as the complex.

Experimental

Hollow capsules were prepared as described in the literature [2]. Monodisperse spheres ($d = 5.94$ mm) of weakly polymerized melamine-formaldehyde resin (Microparticle GmbH) were covered by 4 double layers of PSS (MW 70 000 g mol^{-1}, Aldrich) and PAH (MW 70 000 g mol^{-1}, Aldrich). The resin core was dissolved in 0.1 M hydrochloric acid and the remaining capsules were thoroughly washed with water until pH 6 was reached. The outer layer is PAH and is positively charged. The surface charge was measured by means of a Malvern Zetasizer 3000 Has apparatus.

The filling of the capsules by polystyrene sulfonate was performed by a ship in bottle synthesis of the polymer as described in the literature (see Scheme 1) [6]. Polymerization was carried out at a styrenesulfonate concentration of 0.5 M in the presence of hollow capsules under nitrogen atmosphere according to standard procedures in the literature. As initiator, 1 % potassium peroxodisulfate, related to the monomer concentration, was used. The use of *N*,*N*,*N*′,*N*′-tetramethylethylenediamine as catalyst allowed to perform the polymerization at 40 °C. After polymerization, the capsules were separated from the PSS in the bulk solution by centrifugation. Several washing cycles with water followed.

Absorption spectra were measured using a Varian Cary qe UV-vis spectrophotometer between 200 and 800 nm. Fluorescence spectra were obtained using a Spex Fluorolog 1680 Double Spectrometer. Both excitation and emission bandwidths were set at 1.0 nm. All measurements were performed on air-equilibrated solutions at 25 °C.

The size, integrity, and degree of filling of individual capsules were determined by an inverse CLSM (Leica, Germany) with a 100× oil immersion objective with a numerical aperture of 1.4. The capsules were visualized either by electrostatic adsorption of the fluorescent dye rhodamine 6G to the polyelectrolytes and their complexes or by addition of 1,1′-diethyl-2,2′-cyanine (NK-1046, Nippon Shisiko Kenkyusho, Japan).

Scanning force microscopy (SFM) was applied to capsules air-dried on freshly cleaved mica. SFM images have been recorded in air at room temperature using a Nanoscope III Multimode SFM (Digital Instrument, Santa Barbara, USA) in tapping mode. Microlithographed tips on silicon nitride (Si_3N_4) cantilever with a force constant of 42 N m^{-1} were used. SFM images were processed using a Nanoscope software.

Received: February 13, 2003
Final version: July 17, 2003

[1] H. Auweter, H. Haberkorn, W. Heckmann, D. Horn, E. Luddecke, J. Rieger, H. Weiss, *Angew. Chem. Int. Ed.* **1999**, *38*, 2188.
[2] E. Donath, G. B. Sukhorukov, F. Caruso, S. A. Davis, H. Möhwald, *Angew. Chem. Int. Ed.* **1998**, *37*, 2002.
[3] G. Decher, *Science* **1997**, *277*, 1232.
[4] I. L. Radchenko, G. B. Sukhorukov, S. Leporatti, G. Khomutov, E. Donath, H. Möhwald, *J. Colloid Interface Sci.* **2000**, *230*, 272.
[5] F. Caruso, R. A. Caruso, H. Möhwald, *Science* **1998**, *282*, 1111.
[6] L. Dähne, S. Leporatti, E. Donath, H. Möhwald, *J. Am. Chem. Soc.* **2001**, 5431.
[7] G. B. Sukhorukov, L. Dähne, J. Hartman, E. Donath, H. Möhwald, *Adv. Mater.* **2000**, *12*, 112.
[8] G. Scheibe, *Angew. Chem.* **1936**, *49*, 563.
[9] M. Bednarz, V. A. Malyshev, J. Knoester, *J. Chem. Phys.* **2002**, *117*, 6200.
[10] H. von Berlepsch, C. Böttcher, L. Dähne, *J. Phys. Chem. B* **2000**, *104*, 8792.
[11] C. Peyratout, E. Donath, L. Dähne, *J. Photochem. Photobiol. A* **2001**, *142*, 51.
[12] a) L. Dähne, G. Reck, *Angew. Chem.* **1995**, *107*, 735. b) L. Dähne, G. Reck, *Angew. Chem. Int. Ed. Engl.* **1995**, *34*, 690.
[13] C. Peyratout, E. Donath, L. Dähne, *Photochem. Photobiol. Sci.* **2002**, *1*, 87.

A Low Threshold Polymer Laser Based on Metallic Nanoparticle Gratings**

By *Joachim Stehr*, *Jana Crewett*, *Florian Schindler*, *Ralph Sperling*, *Gero von Plessen*, *Uli Lemmer*, *John M. Lupton*, *Thomas A. Klar*,* *Jochen Feldmann*, *Alexander W. Holleitner*, *Michael Forster*, and *Ullrich Scherf*

Since the demonstration of stimulated emission and optically pumped lasing in organic semiconductors this field of research has gained a considerable amount of interest.[1–5] Apart from an optically amplifying material, the second key ingredient for an organic laser is an optical feedback mechanism. Distributed feedback[6] (DFB) has proven to be particularly useful for organic semiconductor devices as it allows low threshold lasing in thin film waveguide structures. Consequently, DFB has been used as a resonator for optically pumped conjugated polymer lasers.[7–10] However, a severe obstacle to constructing organic diode lasers is the optical loss arising from metallic contacts, which generally outweighs the optical gain. So far, it has been assumed that including a metallic electrode in an organic lasing device would preclude lasing due to a large dissipative energy loss to the metal. Initial gain measurements on metallic electrodes appeared to confirm this.[4] Therefore, most of the DFB structures used to date have been made of non-conducting materials, hence excluding electrically pumped operation. Recently, optically pumped lasing from a polymer DFB laser fabricated directly on top of a silver substrate was shown,[11] however, the lasing threshold was increased to 150 times that of a metal-free device.

In this contribution, we explore a novel strategy for contacting organic injection lasers by depositing the organic semiconductor onto a metallic photonic crystal. Optically pumped las-

[*] Dr. T. A. Klar, J. Stehr, J. Crewett, F. Schindler, R. Sperling, Prof. G. von Plessen,[+] Prof. U. Lemmer,[++] Dr. J. M. Lupton, Prof. J. Feldmann
Photonics and Optoelectronics Group
Department of Physics and CeNS
Ludwig-Maximilians-Universität
Amalienstr. 54, D-80799 München (Germany)
E-mail: thomas.klar@physik.uni-muenchen.de
Dr. A. W. Holleitner
Semiconductor Group, Department of Physics and CeNS
Ludwig-Maximilians-Universität
Schellingstr. 4, D-80799 München (Germany)
Dr. M. Forster, Prof. U. Scherf
FB Chemie, Universität Wuppertal
Gauss-Straße 20, D-42097 Wuppertal (Germany)
[+] Current address: Physikalisches Institut, RWTH Aachen, D-52056 Aachen, Germany.
[++] Current address: Lichttechnisches Institut, Universität Karlsruhe, Kaiserstrasse 12, D-76131 Karlsruhe, Germany.

[**] We are indebted to the DFG for financial support through the Schwerpunkt Photonische Kristalle and the Gottfried-Wilhelm-Leibniz Award, to the BMBF through the OLAS collaboration, and the European Union through the TMR Network HYTEC. We gratefully acknowledge expert technical support from W. Stadler, A. Helfrich, A. Kriele, and K. Werhahn.

  DOI: 10.1002/adma.200305221

ing is demonstrated in a device consisting of a conjugated polymer on top of a two-dimensional (2D) distributed feedback template comprising gold nanodiscs on indium tin oxide (ITO). Although the nanodiscs are potential dissipative energy absorbers, we find only a marginal increase in lasing threshold when compared to conventional dielectric distributed feedback resonators. Using 130 fs pump laser pulses, we find a lasing threshold of only 2 nJ. Our structures also allow an accurate control over the active lasing modes, and provide the possibility of generating two non-degenerate modes of orthogonal polarization in one device.

Our device consists of a glass substrate coated with a 110 nm thick ITO layer which is covered by a 2D grating made out of gold nanodiscs (Fig. 1a). The grating constant is 300 nm and each single nanodisc has a diameter of 110 nm and a height of 30 nm. A ~460 nm thick film of the polymer

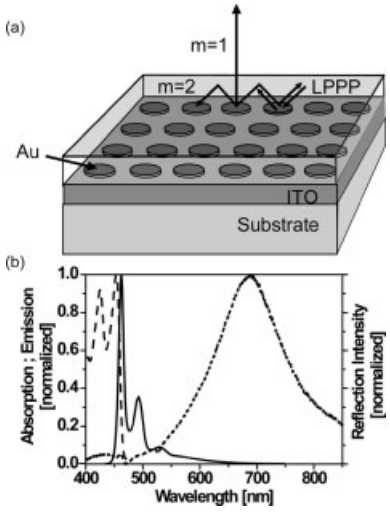

Fig. 1. a) Schematic drawing of the polymer film on top of a gold nanodisc photonic crystal template. Feedback is accomplished by second order ($m = 2$) Bragg scattering, while the first order ($m = 1$) scattering couples the lasing mode out in the vertical direction. The ITO thickness is 110 nm, the gold nanodiscs measure 110 nm in diameter and 30 nm in height, the grating constant is 300 nm and the LPPP film is approximately 460 nm thick. b) Absorption (dashed line) and emission (solid line) spectra of LPPP. Dotted line: Intensity of light reflected by a gold nanoparticle grating not covered by LPPP. The pronounced maximum at approximately 690 nm corresponds to light scattered by the nanoparticle plasmon resonance.

methyl-substituted ladder-type poly(para phenylene) (LPPP) is spin coated onto the sample from toluene solution. Besides offering excellent photophysical properties, this material also has high charge carrier mobilities,[12] which makes it a suitable candidate for electrically pumped laser devices. Figure 1a shows a sketch of the sample and illustrates the DFB mechanism using the second order diffraction for feedback and the first order for coupling the light out perpendicular to the film surface.

The spectral properties of the organic film and the metallic 2D grating can be seen in Figure 1b, where the absorption (dashed line) and emission (solid line) spectra of LPPP are displayed. The light reflected by a similar gold nanoparticle grating without a LPPP film is shown by the dotted line. The pronounced maximum at approximately 690 nm corresponds to light scattered by the nanoparticle plasmon resonance. Note that there is only little overlap between the nanoparticle plasmon resonance and the LPPP fluorescence, and hence fluorescence quenching by resonant energy transfer from excited LPPP molecules to the nanoparticle plasmon is assumed to be small, and lasing should not be affected by the nanoparticle plasmon. In fact, reflection measurements with an LPPP layer show that the plasmon peak shifts approximately 30 nm to the red, further reducing the spectral overlap. Calculations reveal that this sample supports two transverse electric (TE) modes, whereby the first one is predominantly confined within the ITO and the second mode has its main maximum within the LPPP layer and shows a nodal plane close to the ITO–LPPP interface, thus additionally minimizing absorption by the gold nanodiscs.

For optical pumping of the laser structure we use laser pulses of 130 fs duration, 1 kHz repetition rate, and a wavelength of 400 nm. Figure 2a shows the first vibronic sideband of the photoluminescence spectrum for three different excitation pulse energies between 1.5 nJ and 2.7 nJ. While an excitation pulse energy of 1.5 nJ is well below the lasing threshold, at an excitation energy of 1.9 nJ a small peak occurs at 492 nm. We note that the concomitant dip in the fluorescence spectrum is absent. At a pump pulse energy of 2.7 nJ a clear lasing mode is observed. The spectral position of this lasing mode can be tuned either by varying the grating constant or the LPPP film thickness. Below a thickness of 350 nm, however, no laser action is observed.

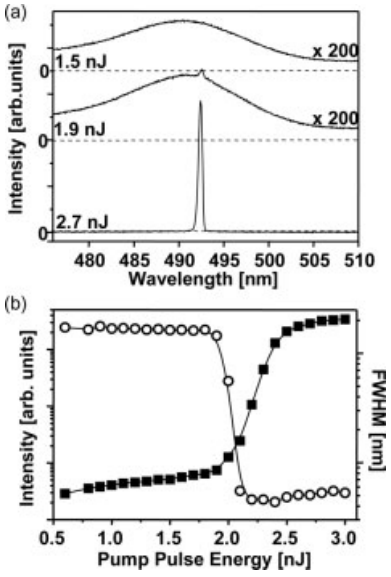

Fig. 2. a) Emission spectrum in the spectral region of the first vibronic sideband of LPPP below, at, and above lasing threshold. The pump pulse energies are indicated. b) Plot of the intensity at the laser wavelength (■) and the FWHM of the emission band (○) against pump pulse energy.

Figure 2b shows the output power at the laser wavelength versus pump energy (solid squares). A clear laser threshold behavior is observed with a threshold energy of approximately 2 nJ. The surprising result is that this lasing threshold

is only a factor of two larger than the lasing threshold for a metal-free LPPP–DFB laser.[9] This is unexpected as the gold nanodiscs are prone to quench molecular excitations via energy transfer to the metal and should therefore increase the laser threshold. One possible reason for this result is that the LPPP emission has little spectral overlap with the nanoparticle plasmon. Further, the second TE mode, which we assume to be the lasing mode, also has little spatial overlap with the gold nanodisc layer. Moreover, in comparison to metal films, the quenching effect of the gold intraband absorption will be strongly reduced since a large part of this kind of absorption in gold nanoparticles is concentrated at the nanoparticle plasmon frequency,[13] and also because the metal filling factor of the nanoparticle array is smaller than that of metal films. Also note that the gold interband absorption at the LPPP emission energy, which is essentially the same in metal nanoparticles and films, is relatively weak and not expected to contribute significantly to the quenching. The full width at half maximum (FWHM) of the emission is also shown as a function of pump energy, which displays a clear laser threshold behavior with the FWHM shrinking down to 0.44 nm at 2.4 nJ pump pulse energy. A subsequent increase in pulse energy results in a slight line broadening to 0.55 nm at 2.9 nJ, which may be due to excitation of further lateral laser modes. This is also manifested in the saturation behavior of the peak count rate.[10]

Our nanolithographic technique provides a simple route for controlling the 2D gain mechanism in the laser. By inducing a slight mismatch of 1 % between the horizontal and vertical grating period, it is possible to spectrally separate the two gain directions. This is shown in Figure 3, where two distinct laser modes are observed at 492 and 495 nm. Surprisingly, the two modes exhibit identical threshold behavior as seen in the right-hand inset. Both laser lines are fully polarized and emit at orthogonal polarizations, as seen in the left inset, which shows the polarization dependence of the two emitted laser lines. We note that an independent selection of the lasing wavelength and the plane of polarization on a single microlaser could have potential applications in optical communications.

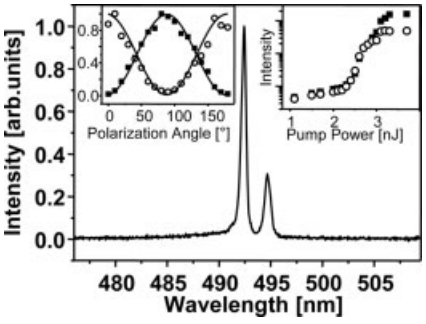

Fig. 3. Dual band lasing resulting from a 1 % mismatch of the period of one grating axis with respect to the other. The two peaks at 492 nm (■) and 495 nm (○) are fully polarized orthogonal to each other (left inset) and exhibit identical threshold behavior (right inset).

Next, we address the question of the feedback mechanism in our device. Feedback by DFB structures can in principle be established by index-coupling, by gain coupling, or a superposition of both resulting in complex coupling. The absence of a stop band in the sub-threshold luminescence spectrum suggests that index coupling only plays a marginal role.[10] This is understandable, as the gold nanodiscs are only 30 nm in height, so the light mode is confined predominantly to the spatially unmodulated LPPP film. We therefore have to consider the imaginary part of the coupling constant as the source of the feedback. At this point of research it is hard to tell whether gain or loss coupling dominates. Usually, in second order feedback DFB devices the loss is facilitated by first order Bragg scattering into radiation modes. In the case of the gold nanodisc template used in this study, another important mechanism has to be taken into account, namely absorption by the gold nanodiscs. Gold nanoparticles have been shown to be extremely effective fluorescence quenchers,[14] and therefore the quenching processes due to the presence of the gold nanodiscs, which should extend well into the LPPP layer, may contribute substantially to the feedback mechanism.[15] In a sense, this could be called a type of "loss" coupling. It is therefore, possible that our laser operates on a combination of gain and "loss" coupling, which would have the same periodicity, whereas conventional lasers usually rely on index coupling. Further research is needed to distinguish between these different coupling mechanisms, but the present results do suggest alternative routes to achieving feedback and gain in organic semiconductors.

Our findings are promising results towards the realization of future organic injection lasers. The metallic nanoparticle grating in our work not only serves as a means for providing optical feedback but may also act as a cathode in an electrically driven device. As an anode a suitable low-loss metal film has to be evaporated. Alternatively, ITO can also be used as the second contact when an additional electron injection layer is introduced.[16] Depending on the relative positions of the workfunctions of the ITO layer and the Au discs (depending on the treatment of the former), as well as the operating conditions, hole injection will occur either over the entire contact or at isolated areas. Concomitantly, this will determine the relative importance of gain and index modulation. Further work has to address these issues. Novel lithographic techniques for creating metallic nanostructures based on self-assembly of organic nanospheres[17] may provide a facile method for structuring the electrode as well as enabling the production of large area gratings.

In summary, we have shown that a 2D photonic crystal of gold nanodiscs on ITO can be used as a DFB substrate for organic lasers. Contrary to expectation, the metal does not increase the threshold for lasing significantly compared to purely dielectric gratings, suggesting a method for contacting thin films of organic semiconductors.

Experimental

The gold nanodisc grating has a total size of 96 μm × 96 μm and is produced by electron beam lithography. Each single nanodisc has a diameter of 110 nm and a height of 30 nm. The grating constant is 300 nm. A film of LPPP is spin

coated onto the sample from toluene solution. The average film thickness as determined from optical density measurements is 460 ± 20 nm.

For optical pumping of the laser structure we frequency double the output of a regeneratively amplified femtosecond Ti:Sapphire laser. The resulting pulses of 130 fs duration and a wavelength of 400 nm have pulse energies of 0.6 nJ to 10 nJ at a repetition rate of 1 kHz. The excitation beam is focused onto a spot with a diameter of 70 ± 5 μm. The sample is kept under a dynamic vacuum of 10^{-4} mbar and the emission is collected in reflection geometry, dispersed by a grating spectrometer and detected by a charge coupled device (CCD) array.

Received: April 3, 2003
Final version: July 8, 2003

[1] F. Hide, M. A. Diaz-Garcia, B. J. Schwartz, M. R. Andersson, P. Qibing, A. J. Heeger, *Science* **1996**, *273*, 1833.
[2] N. Tessler, G. J. Denton, R. H. Friend, *Nature* **1996**, *382*, 695.
[3] S. V. Frolov, W. Gellermann, M. Ozaki, K. Yoshino, Z. V. Vardeny, *Phys. Rev. Lett.* **1997**, *78*, 729.
[4] M. D. McGehee, A. J. Heeger, *Adv. Mater.* **2000**, *12*, 1655.
[5] V. G. Kozlov, G. Parthasarathy, P. E. Burrows, V. B. Khalfin, J. Wang, S. Y. Chou, S. R. Forrest, *IEEE J. Quantum Electron.* **2000**, *36*, 18.
[6] C. V. Shank, J. E. Bjorkholm, H. Kogelnik, *Appl. Phys. Lett.* **1971**, *18*, 395.
[7] C. Kallinger, M. Hilmer, A. Haugeneder, M. Perner, W. Spirkl, U. Lemmer, J. Feldmann, U. Scherf, K. Müllen, A. Gombert, V. Wittwer, *Adv. Mater.* **1998**, *10*, 920.
[8] M. D. McGehee, M. A. Díaz-García, F. Hide, R. Gupta, E. K. Miller, D. Moses, A. J. Heeger, *Appl. Phys. Lett.* **1998**, *72*, 1536.
[9] S. Riechel, C. Kallinger, U. Lemmer, J. Feldmann, A. Gombert, V. Wittwer, U. Scherf, *Appl. Phys. Lett.* **2000**, *77*, 2310.
[10] S. Riechel, U. Lemmer, J. Feldmann, T. Benstem, W. Kowalsky, U. Scherf, A. Gombert, V. Wittwer, *Appl. Phys. B* **2000**, *71*, 897.
[11] P. Andrew, G. A. Turnbull, I. D. W. Samuel, W. L. Barnes, *Appl. Phys. Lett.* **2002**, *81*, 954.
[12] D. Hertel, U. Scherf, H. Bässler, *Adv. Mater.* **1998**, *10*, 1119.
[13] U. Kreibig, M. Vollmer, *Optical Properties of Metal Clusters*, Springer, Berlin **1995**.
[14] E. Dulkeith, A. C. Morteani, T. Niedereichholz, T. A. Klar, J. Feldmann, S. A. Levi, F. C. J. M. Van Veggel, D. N. Reinhoudt, M. Möller, D. I. Gittins, *Phys. Rev. Lett.* **2002**, *89*, 203 002.
[15] M. Kamp, J. Hofmann, A. Forchel, F. Schäfer, J. P. Reithmaier, *Appl. Phys. Lett.* **1999**, *74*, 483.
[16] G. Parthasarathy, P. E. Burrows, V. Khalfin, V. G. Kozlov, S. R. Forrest, *Appl. Phys. Lett.* **1998**, *72*, 2138.
[17] M. C. Netti, S. Coyle, J. Baumberg, M. A. Ghanem, P. R. Birkin, P. N. Bartlett, D. M. Whittaker, *Adv. Mater.* **2001**, *13*, 1368.

A Novel Approach for Preparation of Thermoresponsive Polymer Magnetic Microspheres with Core–Shell Structure**

By *Yonghui Deng*, *Wuli Yang*, *Changchun Wang*, and *Shoukuan Fu**

In the past decades, there has been great interest in the fabrication of stimuli-responsive polymer microspheres for technological applications and fundamental studies. Due to their ability to change physical–chemical properties and colloidal properties in response to external stimuli (changes in temperature, pH, ionic strength, magnetic field, etc.),[1] stimuli-responsive polymer microspheres have many versatile applications, especially in biomedical and biotechnological fields such as drug-delivery systems, specific molecular recognition, biosensors, affinity separations, enzyme and cell immobilizations, etc.[2] Among stimuli-responsive polymer microspheres, thermoresponsive polymer microspheres, particularly those based on poly(*N*-isopropylacrylamide) (PNIPAM), have attracted much attention and were intensively investigated since poly(*N*-isopropylacrylamide) microgel particles were first reported by Pelton and Chibante in 1986.[1a] Poly(*N*-isopropylacrylamide) is a well-known thermoresponsive polymer, which exhibits a coil–globule transition in aqueous solution at a lower critical solution temperature (LCST) of about 32 °C.[3] Thermoresponsive polymer microspheres based on poly(*N*-isopropylacrylamide) have been applied to several different fields, such as nucleic-acid extraction and purification,[4] controlled release,[5] and cell-culture substrates.[6]

More recently, with the development of the preparation and application of stimuli-responsive polymer microspheres, increasing interest has been devoted to the exploration of multiresponsive polymer microspheres, which exhibit sensitivity to several external stimuli and can be used in extended fields. Polymer microspheres that combine both temperature- and pH-responsive volume phase transitions were elaborated as reported by many authors.[7] Owing to their relatively rapid and easy magnetic separation, thermoresponsive polymer magnetic microspheres could be widely used in biomedical and bioengineering, such as enzyme immobilization and immunoassay, cell separation, and clinical diagnosis. In addition, due to their sensitivities to both magnetic field and temperature, thermoresponsive polymer magnetic microspheres offer a high potential application in the design of a targeting drug-delivery system, which is considered as a safe and effective way for tissue-specific release of drugs, i.e., with a small amount of magnetic thermoresponsive polymer microspheres, a large amount of drug could be easily administered and transported to the site of choice. Under the guidance of an external magnetic field, such dual-responsive polymer microspheres could arrive at the specific tissue and release drugs loaded on the microspheres at the targeting spot using temperature as a trigger.

Micrometer- and submicrometer-sized thermoresponsive polymer magnetic microspheres based on a copolymer of styrene and *N*-isopropylacrylamide has been synthesized previously. Sauzedde et al.[8a] reported on the preparation of magnetic thermoresponsive microspheres using a two-step method, in which iron-oxide nanoparticles were absorbed onto previously synthesized poly(*N*-isopropylacrylamide-*co*-styrene) microspheres, and then the obtained microspheres were encapsulated by PNIPAM through a soap-free polymerization process. Although this two-step method could lead to thermoresponsive polymer magnetic composite microspheres, the process of preparation is not easily controllable. Ding et al.[8b] prepared thermoresponsive polymer magnetic microspheres based on the dispersion copolymerization of styrene

[*] Prof. S. K. Fu, Y. H. Deng, Dr. W. L. Yang, Prof. C. C. Wang
Department of Macromolecular Science and
Key Laboratory of Molecular Engineering of Polymers
Ministry of Education, Fudan University
Shanghai 200433 (China)
E-mail: skfu@srcap.stc.sh.cn

[**] We are grateful to the support of the State High Technology Development Program 863(2001AA218011).

 DOI: 10.1002/adma.200305459